Three-Dimensional Local Yield Maps of Hard Coating Under Sliding Contact

P. Y. Zhang

D. F. Diao[1]
e-mail: dfdiao@mail.xjtu.edu.cn

Key Laboratory of Education Ministry
for Modern Design and Rotor-Bearing System,
School of Mechanical Engineering,
Xi'an Jiaotong University,
Xi'an 710049, P. R. C.

Z. J. Wang
State Key Laboratory of
Mechanical Transmission,
Chongqing University,
Chongqing 400030, P. R. C.

The local yield maps for the identification of the yield initiation positions of hard coating on three-dimensional (3D) elastic half space under sliding contact were developed. In this study, the semi-analytical method (SAM), which is based on the conjugate gradient method (CGM) and the discrete convolution and fast Fourier transform (DC-FFT) technique, was employed to analyze the contact problem. By using this method, the von Mises stress distributions for various combinations of coating thicknesses, friction coefficients, and elastic moduli of the coating and substrate were calculated. Then, the positions of yield initiation were found with the calculated results by comparing the critical maximum contact pressure $P_{max,c}$ for von Mises yielding at or in the different positions (surface, coating, interface, and substrate), and the 3D-local yield maps were introduced in relation to the yield strength ratio of the coating to the substrate (Y_f/Y_b) and the ratio of the coating thickness to the Hertzian contact radius (t/a_0). Finally, the effect of critical friction coefficient on the transition of yielding positions was discussed.
[DOI: 10.1115/1.4005265]

Keywords: local yield map, hard coating, sliding contact, friction coefficient, yield strength ratio

1 Introduction

The progress of coating technology is the reason for the wide employment of hard coatings to improve the tribological properties of contact surfaces. For many industrial applications, hard coatings can significantly offer a low friction coefficient, enhanced counterpart protection, high wear resistance, and corrosion resistance [1–5]. From the view of the engineering application of hard coating, it is well known that fractures in the coating (cohesive failure) or delamination and spalling (adhesive failure) at the interface between coating and substrate are the weak points of the hard coating in use [6–10]. In many cases, micro-cracks exist at the surface and interface in thin coatings, and large cracks are propagated from there. But interfacial cracks are more likely to be initiated in thinner coatings as a result of mismatch of the coating and the substrate properties and are due to the location of maximum shear stress at the coating-substrate interface [11–15]. Recently, Zhou et al. [16] studied the spalling wear behavior of hard coatings, and they showed that the spalling wear particle depends on the depths of pre-existing cracks, the positions of the cracks relative to major surface asperities, and loading conditions. Thus, the critical contact condition for the propagation of a crack becomes the main concern in the design of coating. For this purpose, it is the first approach to know the critical contact condition for the local yield initiation through the stress distribution in the contact region. Therefore, it is quite important to find and control the yielding initiation to prevent the delamination or the spalling.

In layered contact problems, the calculations of von Mises stress distributions are essential for the studies of the plastic flow, crack, or delamination. Nowell and Hills [17] investigated elastic contact between the cylinder and a rigid frictionless substrate under normal and tangential loads, but their investigations were limited to the line contact problem. O'Sullivan and King [18] analyzed 3D quasi-static stress states by using the least-squares approach and determined the distributions of von Mises stresses in the coating and substrate. It was found that the position of the maximum von Mises stress depends on the stiffness of the coating relative to the substrate, the ratio of coating thickness to contact radius, and the value of the coefficient of friction. Komvopoulos et al. [19–21] studied the elastic contact problem of a layered semi-infinite solid compressed by a rigid surface with the finite element method (FEM) numerically. They also solved the elastic-plastic contact problem in a similar situation, showing that yielding in the layered medium always initiates at the coating-substrate interface below the center of the contact, and the plastic zone does not grow toward the surface of the indented layered medium but is restricted to the boundary of the hard coating and the substrate. Plumet and Dubourg [22] presented a numerical 3D contact model between the elastic multilayered body and rigid body to guide choice among coating/substrate combinations that can withstand the applied loads. This model was able to solve the contact problem under partial slip, rolling/sliding contact conditions and to determine the subsurface stress field. Stephens et al. [23] investigated the initial yielding behavior of a coating/functionally graded substrate system under indentation and friction, and their results clearly showed distinct benefits by a functional gradient in yield strength and/or in elastic modulus of the substrate to the reliability of coated systems. Failure mechanisms of the substrate and coating composite were studied in Michler and Blank's paper [24] through a parametric elastic-plastic finite element analysis (FEA) for the common load case of the indentation of spherical bodies into a layered surface considering a wide range of coating thicknesses. Their results were summarized in normalized failure maps, from which the optimal coating thickness for the special load case of a spherical indentor can be estimated. Holmberg et al. [25] developed a 3D-FEM model to present a tribological analysis of deformations and stresses generated and their influences on crack generation and fracture in a layered surface loaded by a sliding sphere in dry conditions. In recent years, a number of researchers have also applied the boundary element method (BEM) [26,27] and the semi-analytical method to analyze cracks numerically in layered elastic solids [28]. Furthermore, the conjugate gradient method (CGM) [29,30] and the discrete convolution and fast Fourier transform technique [31] were utilized to reduce the computing time for solving contact problems. By using CGM and DC-FFT techniques, Boucly et al. [32] studied contact analyses for bodies with frictional heating and plastic behavior, Wang et al. [33] investigated the partial slip contact problem on

[1]Corresponding author.

Contributed by the Tribology Division of ASME for publication in the JOURNAL OF TRIBOLOGY. Manuscript received June 18, 2011; final manuscript received September 28, 2011; published online March 6, 2012. Assoc. Editor: Daniel Nélias.

three-dimensional layered materials, and Chen et al. [34] studied the elasto-plastic indentation on layered materials using the equivalent inclusion method and given the yielding and plastic zone expansion behavior. On the other hand, Diao et al. [35–38] proposed the two-dimensional (2D) local yield map for the indentation and friction of a coating-substrate system under sliding contact, whose study showed clearly that the ratio of the yield strength of the coating to the substrate, the ratio of the coating thickness to the Hertzian contact radius, and the friction coefficient play an important role in controlling the position of yielding. However, to our best knowledge, the local yield map of hard coating under both normal and tangential loads on three-dimensional elastic half space has not been developed in the open literatures.

Thus, the purpose of this paper is to develop the 3D-local yield maps of hard coating under sliding contact on elastic half space. In this study, a SAM, which is based on the CGM and DC-FFT techniques, was employed to analyze the contact problem in this tribosystem. By using this method, the von Mises stress distributions for various combinations of coating thicknesses, friction coefficients, and elastic modulus of the coating and substrate were calculated. According to the results of simulation, the positions of yield were found. Moreover, 3D-local yield maps were plotted as a similar way from those of the 2D-local yield maps [35,36], which is related to the yield strength ratio of the coating to the substrate (Y_f/Y_b) and the radio of the coating thickness to the Hertzian contact radius (t/a_0).

2 Three-Dimensional Elastic Contact Model

The current model, as shown in Fig. 1, is used to analyze the sliding contact between a rigid ball and a smooth flat with a layer of coating. The coating is perfectly bonded to an elastic substrate, and it has a uniform thickness t. Normal load W and tangential forces F_x are both applied on the rigid ball. The direction of surface tractions corresponds to that of traction applied on the half space. The contact initially takes place at the origin point. In the figure, a denotes the actual radius of the contact zone. In the coordinate system shown in Fig. 1, the surface of coating and the interface between coating and substrate are defined as $z=0$ and $z=t$, respectively.

The calculation parameters are given in Table 1. Normal load was fixed and tangential load F_x was increased with the friction coefficient μ changed from 0.00 to 0.70. A representative combination for the hard coating given by the Young's modulus value E_f of coating 420 GPa, and the Young's modulus value E_b of substrate 210 GPa, was selected. So the Young's modulus ratio of the coating to the substrate was kept constant at two for simulating the ceramic coating layered metal substrate in practice. Poisson's ratio was taken as 0.3 for both the coating and substrate. P_0 and a_0 are the maximum Hertzian contact pressure and Hertzian contact radius with uncoated condition, respectively. The value of t/a_0 was changed from 0.125 to 4.0. The computational domain was specified as $-2a_0 < x < 2a_0$, $-2a_0 < y < 2a_0$, and $0 < z < 8a_0$. In

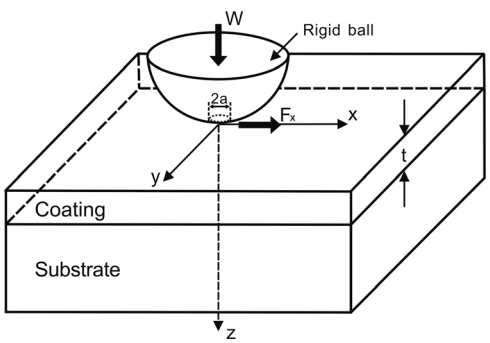

Fig. 1 The model of a rigid ball and a layered substrate in sliding contact

Table 1 Calculation parameters

Parameters	Value
Load, W (N)	20
Friction coefficient, μ	0.00, 0.25, 0.50, 0.70
Tangential load, F_x(N)	μW
Ball radius, R (mm)	18
Young's modulus of coating, E_f (GPa)	420
Young's modulus of substrate, E_b (GPa)	210
Possion's ratio of coating, ν_f	0.3
Possion's ratio of substrate, ν_b	0.3
Maximum Hertzian pressure, P_0 (MPa)	860.03
Hertzian contact radius, a_0 (mm)	0.10537
Thickness of coating, t (mm)	(0.125, 0.5, 1.0, 1.5, 1.75, 2.0, 2.5, 3.0, 3.5, 4.0) × a_0

the following analysis, the stresses were normalized by P_0, and the coordinates were normalized by a_0.

This contact problem in the model above was solved by using a SAM, in which CGM and DC-FFT techniques were employed to increase the solution speed. Wang, one of the authors for this paper, has given a detailed description of this method in the previous study [33]. In this paper, we applied the method to obtain the results of the von Mises stresses in a hard coating under normal and tangential loads and discussed plotting the 3D-local yield maps under different conditions with various material properties and coating thicknesses.

3 Calculation Results

3.1 Distributions of the von Mises Stress. The position of yield in the coating and substrate is governed by the von Mises stress $\sqrt{J_2}/P_0$, where J_2 is the second invariant of the stress deviator tensor [18]. First, the elastic properties of the coating and substrate were the same. The contours of the dimensionless von Mises stress in the plane $y=0$, calculated from the sliding contact model with different friction coefficients from 0.00 to 0.70, are plotted in Fig. 2. In the case of $\mu=0.00$, as shown in Fig. 2(*a*), the maximum von Mises stress is 0.362, which has the small difference of 0.968% compared with the result in O'Sullivan and King's investigation (see Ref. [18]). Similar small differences can be obtained when $\mu=0.25$ or $\mu=0.50$. Despite some differences, our results are in good agreement with the Ref. [33]. Under the condition of non-layered status, the results show that the position of the maximum von Mises stress is located below the surface or contact center for relatively low friction. When the friction coefficient is increased (see Figs. 2(*c*)–2(*d*)), the maximum von Mises stress appears on the contact surface.

Then, we focused on the sliding contact of hard coatings. Figures 3–4 show the contour plots of the von Mises stress $\sqrt{J_2}/P_0$ in the $y=0$ plane for $\mu=0.00$ and $\mu=0.25$ but with different coating thicknesses. For $\mu=0.25$, in the case of $t=0.125a_0$, the maximum von Mises stress occurs at the surface of the coating. For $t=0.5a_0$, the maximum stress with a mild discontinuity occurs at the interface. And if the coating thickness is increased from $t=a_0$ to $t=2a_0$, it can be seen clearly that the position of the maximum stress moves upward in the coating. When the friction coefficient is increased, as shown in Figs. 5–6, the maximum von Mises stress is always located at the surface.

3.2 3D-Local Yield Map. It has been mentioned in the previous studies of Diao et al. that the critical maximum contact pressure $P_{max,c}$ for von Mises yielding were obtained from Refs. [35–38].

$$P_{max,c} = Min[Y(x,0,z)/\psi_Y(x,0,z)] \quad (1)$$

Here, $\psi_Y(x, 0, z)$ is the ratio of maximum von Mises stress to maximum Hertzian contact pressure $\sigma_{vm,max}/P_0$, and $Y(x, 0, z)$ is the

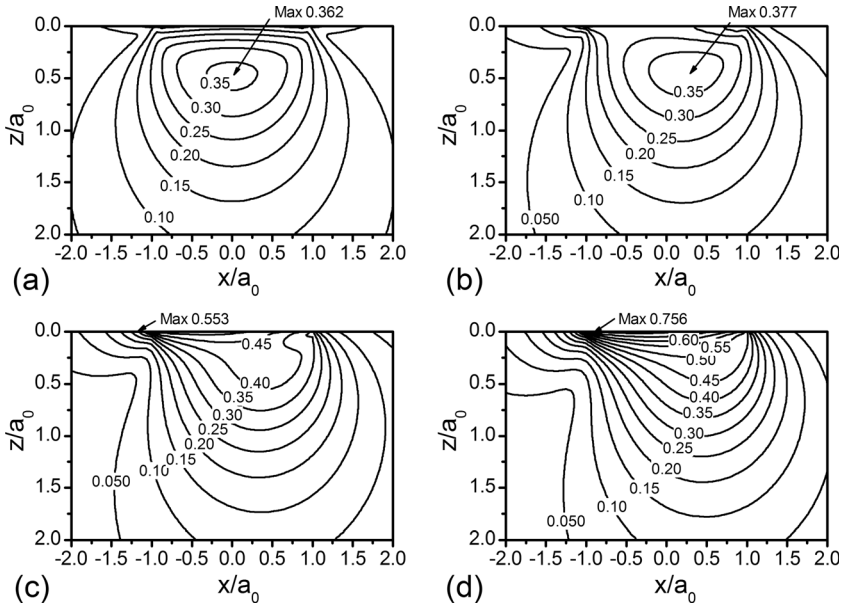

Fig. 2 Contour plots of the von Mises stress $\sqrt{J_2}/P_0$ in the y = 0 plane for $E_f/E_b = 1$; (*a*) $\mu = 0.00$, (*b*) $\mu = 0.25$, (*c*) $\mu = 0.50$, (*d*) $\mu = 0.70$

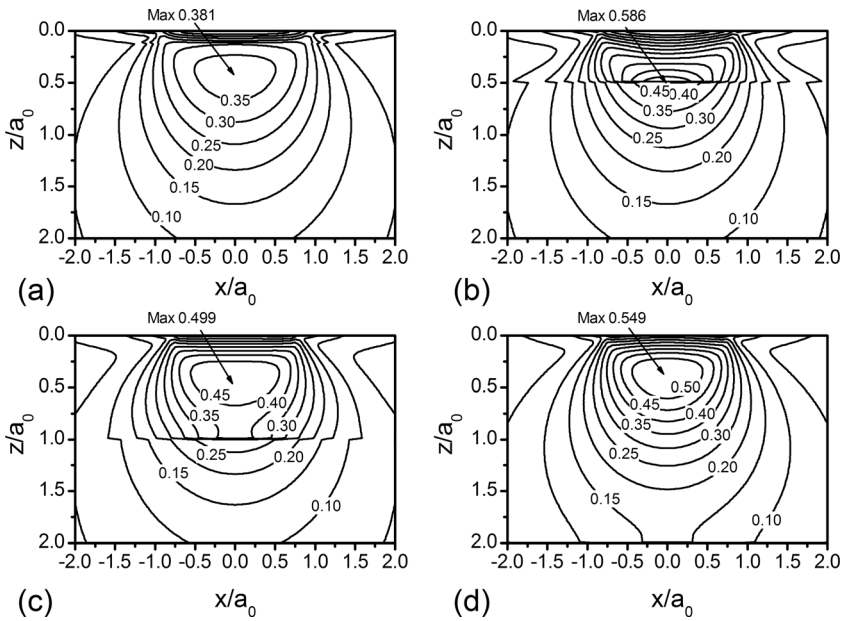

Fig. 3 Contour plots of the von Mises stress $\sqrt{J_2}/P_0$ in the y = 0 plane for $E_f/E_b = 2$ and $\mu = 0.00$; (*a*) $t = 0.125a_0$, (*b*) $t = 0.5a_0$, (*c*) $t = a_0$, (*d*) $t = 2a_0$

distribution of the yield strength in the y = 0 plane. In this study, $Y(x, 0, z)$ only depends on the value of z, when $z < t$, $Y(x, 0, z) = Y_f$, and when $z > t$, $Y(x, 0, z) = Y_b$, where Y_f and Y_b are the yield strength of the coating and substrate materials, respectively. Only the case of $Y_f > Y_b$ is included by considering the hard coating under sliding contact in this paper, so the yield condition at the interface can be given by $Y(x, 0, z) = Y_b$. The relationship between $\sigma_{vm,max}/P_0$ and t/a_0 for several friction coefficient μ values is shown in Fig. 7, where ψ_s, ψ_f, ψ_i, and ψ_b are the values of $\psi_Y(x, 0, z)$ at the surface, in the coating, at the interface, and in the substrate, respectively. As can be seen in Fig. 7(*b*), the values of ψ_s, ψ_f, ψ_i, and ψ_b keep a complicated manner depending on the value of t/a_0. When t/a_0 is smaller than 0.5, the value of $\sigma_{vm.max}/P_0$ at the surface is larger than any others. If the value of t/a_0 is increased from 0.5, the value of $\sigma_{vm.max}/P_0$ in the coating is always larger than that at the surface, and the value of $\sigma_{vm.max}/P_0$ at the interface is always larger than in the substrate. When the friction coefficient becomes larger, as shown in Figs. 7(*c*)–7(*d*), the maximum value no longer appears in the coating, the value of $\sigma_{vm,max}/P_0$ at the surface is the largest of all while the value of that in the substrate is the smallest.

By substituting values of ψ_s, ψ_f, ψ_i, and ψ_b at a certain value of t/a_0 in Fig. 7 and the yield strength corresponding to these values of $\psi_Y(x, 0, z)$ in the y = 0 plane into Eq. (1) respectively, the smallest value of $P_{max,c}$ and the position for yielding under the given friction coefficient can be found. The positions of yield initiation were decided in this way for the given coating thicknesses and friction conditions.

As shown in Figs. 8–9, the positions of yield initiation were investigated for the case $\mu = 0.00$, $\mu = 0.25$, $\mu = 0.50$, and

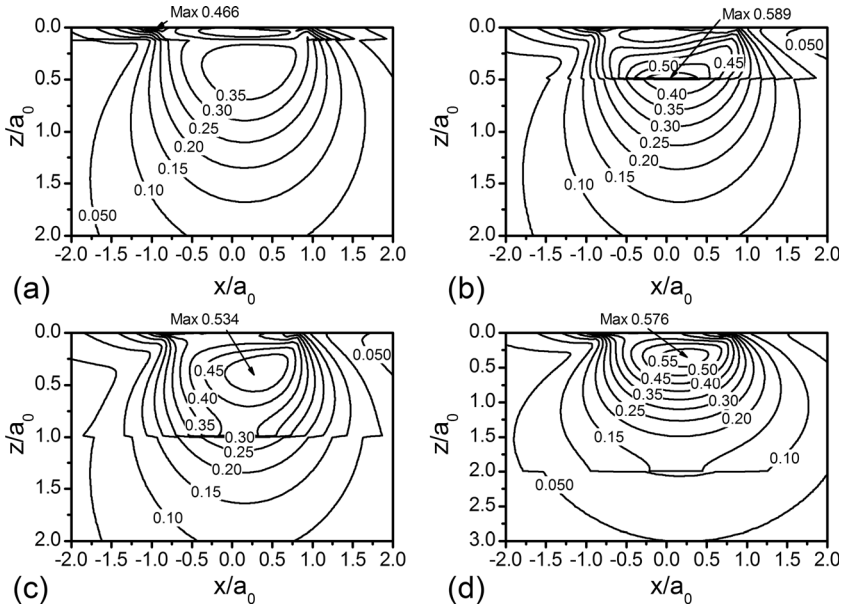

Fig. 4 Contour plots of the von Mises stress $\sqrt{J_2}/P_0$ in the y = 0 plane for $E_f/E_b = 2$ and $\mu = 0.25$; (*a*) $t = 0.125a_0$, (*b*) $t = 0.5a_0$, (*c*) $t = a_0$, (*d*) $t = 2a_0$

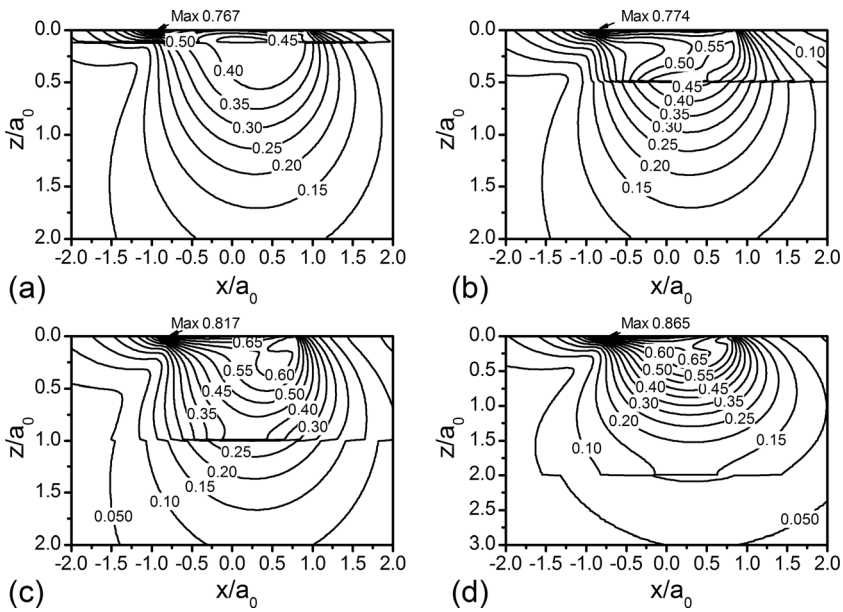

Fig. 5 Contour plots of the von Mises stress $\sqrt{J_2}/P_0$ in the y = 0 plane for $E_f/E_b = 2$ and $\mu = 0.50$; (*a*) $t = 0.125a_0$, (*b*) $t = 0.5a_0$, (*c*) $t = a_0$, (*d*) $t = 2a_0$

$\mu = 0.70$. 3D-local yield maps were introduced in relation to the yield strength ratio of the coating to the substrate (Y_f/Y_b) and the ratio of the coating thickness to the Hertzian contact radius (t/a_0). In 3D-local yield maps, Y_f/Y_b is varied between 1 and 7, t/a_0 is varied between 0 and 4 and the value of E_f/E_b is kept constant at 2. Full lines are tentatively drawn as boundaries between two different yield position regions. It is worthy of careful observation that the position of the oval mark in the models of the map represents where the yield first occurs.

For non-surface friction or relatively low friction, as shown in Figs. 8(*a*) and 8(*b*), the yield in the coating dominates in all cases when t/a_0 is greater than three. Moreover, the yield in the substrate dominates in almost all cases of Y_f/Y_b when t/a_0 is smaller than about 0.25, which is consistent with the results in 2D-local yield maps (see Refs. [35,36]). However, if the value of t/a_0 is smaller than 0.25 and the friction coefficient is 0.25, the yield will occur at the surface as we move the value of Y_f/Y_b from 1 to 1.25 (see Fig. 8(*b*)). This is because the relatively thin hard coating brings a high stress arising at the surface (see Fig. 7(*b*)). Note that this phenomenon will not appear for relatively low friction coefficients in 2D-local yield maps. As shown in Figs. 8(*b*) and 9(*a*), if the friction coefficient is increased from 0.25 to 0.50, the possibility of surface yield increases while the yield in the coating and substrate decreases, and finally the yield in the coating and substrate disappears (see Fig. 9(*a*)). In addition, the value of t/a_0 is over 2.0, local yield appears at the surface under a wide variety of Y_f/Y_b values, and the yield at the interface dominates as the value of t/a_0 is smaller than about 1 for most cases of Y_f/Y_b (see Figs. 9(*a*) and 9(*b*)). Also, the 3D-local yield maps show that the yield at the coating-substrate interface disappears when t/a_0 is greater than about 2.5, which is quite different with those from 2D-local yield maps. It may be generally concluded from Figs. 8–9 that if the

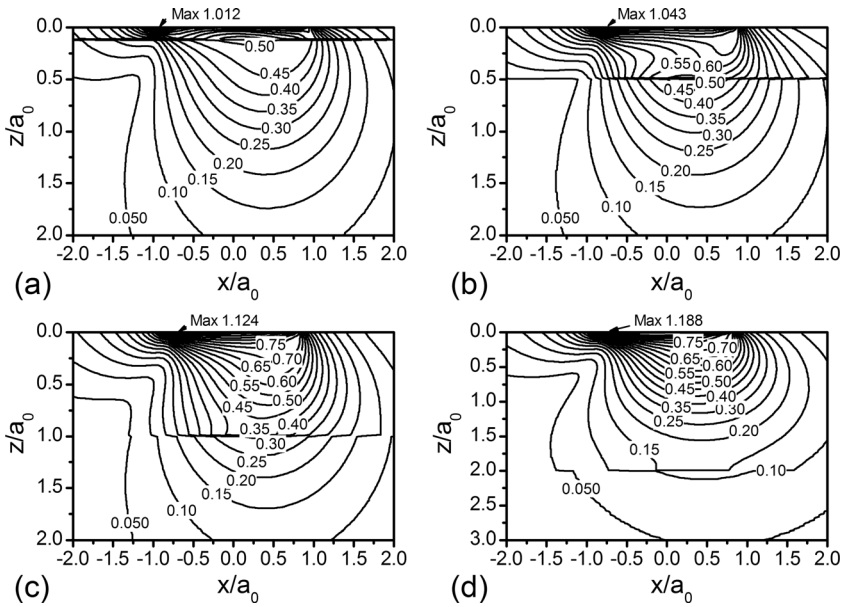

Fig. 6 Contour plots of the von Mises stress $\sqrt{J_2}/P_0$ in the y = 0 plane for $E_f/E_b = 2$ and $\mu = 0.70$; (*a*) $t = 0.125a_0$, (*b*) $t = 0.5a_0$, (*c*) $t = a_0$, (*d*) $t = 2a_0$

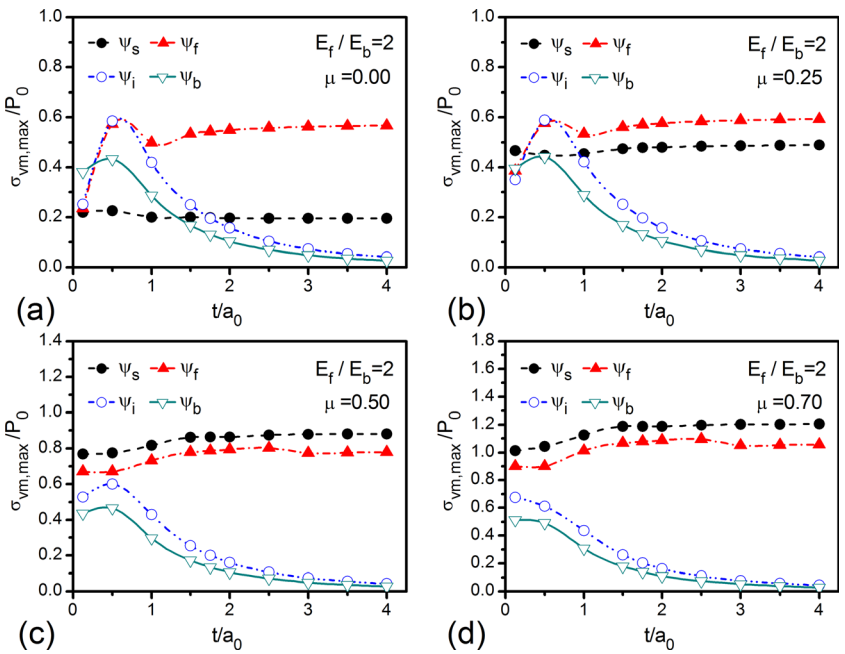

Fig. 7 Relationship between $\sigma_{vm,max}/P_0$ and t/a_0 for $E_f/E_b = 2$; (*a*) $\mu = 0.00$, (*b*) $\mu = 0.25$, (*c*) $\mu = 0.50$, (*d*) $\mu = 0.70$

friction coefficient is increased from 0.50 to 0.70 and the value of t/a_0 is over 2.5, the possibility of yield at the surface dominates instead of in the coating. However, if the friction coefficient is smaller than 0.25, the yield in the coating or in the substrate will occur.

4 Discussion

According to 3D-local yield maps, the interface and the surface are two main possible sites for local yield initiation under various frictional conditions, which agrees with our preceding research results [35,36]. Therefore, the initial defects such as micro-cracks at the interface and the surface become important as stress concentration sources which lead to wear. In the real tribosystem with layered elements, either the interface or the surface should be treated more carefully to avoid the crack propagation. So it is necessary to evaluate the critical maximum contact pressure $P_{max,c}$ for the yield at the interface and surface.

Figures 10(*a*) and 10(*b*) show the results of $P_{max,c}$. Here, H_b is the hardness of the substrate, H_f is the hardness of the coating, and $H_b = 3Y_b$ and $H_f = 3Y_f$ are assumed. It should be emphasized that the hardness of substrate and coating is easier to measure than yield strength, and $Y_f/Y_b = H_f/H_b$ is widely accepted in practical application. Therefore, the hardness of substrate and coating to normalize $P_{max,c}$ was used and $H_b = 3Y_b$, $H_f = 3Y_f$ were selected as a representative combination for the hard coating. According to these two figures and Eq. (1), we can control the occurrence of the yield at the interface and the surface. At the same time, if the yield occurrence at the interface or at the surface can be controlled, then the crack initiation there should be prevented.

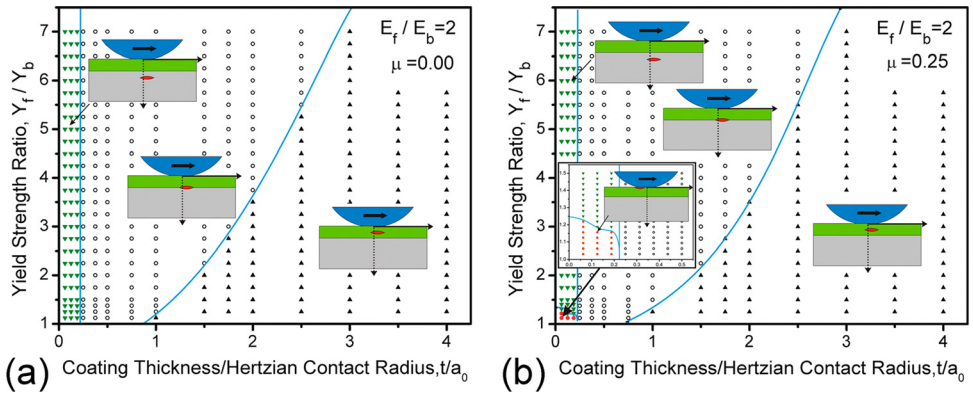

Fig. 8 3D-local yield maps of hard coating for low friction coefficients under sliding contact, (*a*) $\mu = 0.00$ and (*b*) $\mu = 0.25$

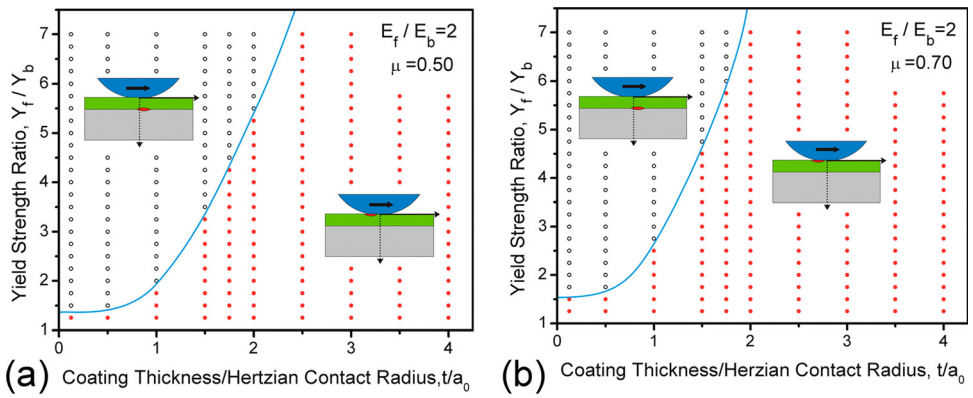

Fig. 9 3D-local yield maps of hard coating for high friction coefficients under sliding contact, (*a*) $\mu = 0.50$ and (*b*) $\mu = 0.70$

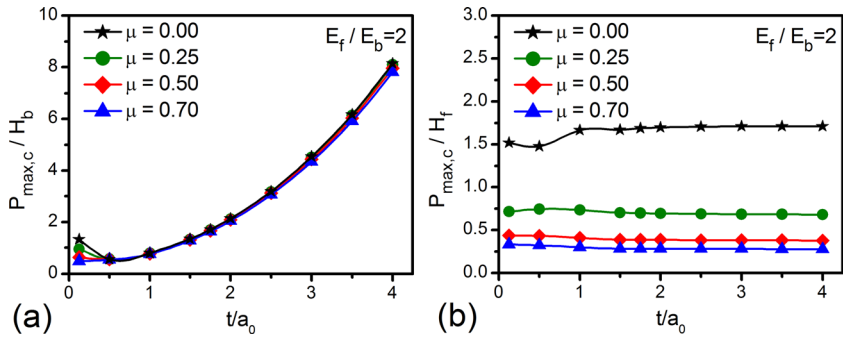

Fig. 10 Critical maximum contact pressure $P_{max,c}$ for the yield, (*a*) at the interface and (*b*) at the surface

It can be summarized from Fig. 10 and our previous studies [35,36] that (1) to obtain a higher maximum critical contact pressure for the yield at the interface, increasing the substrate hardness H_b and the ratio value of the coating thickness to the Hertzian contact radius t/a_0 is more effective than the friction coefficient μ when t/a_0 is larger than 0.5; and (2) to prevent yielding at the surface, choosing a relatively lower friction system or increasing the yield strength ratio of the coating to the substrate (Y_f/Y_b) is effective.

It should be pointed out that we have done similar work in obtaining 3D-local yield maps of hard coating for $1 < E_f/E_b \leq 8$, and the results were in agreement with those shown in our paper. The only difference is that the size of the yield zone. This shows that 3D-local yield maps of hard coating for $E_f/E_b = 2$ is practical. For example, when $1 < E_f/E_b < 2$, four yield zones are still kept in Fig. 8(*b*), although the size of the surface yield zone becomes smaller.

It should be also pointed out that in this paper we emphasized the cases of $\mu = 0.00$, 0.25, 0.50, and $\mu = 0.70$ for a group of representative data. For 3D-local yield maps of $0 < \mu < 1$, we give the idea for discussing the effect of critical friction coefficient on the initiation of the yield zone, especially, the transition among local yield maps shown in Figs. 8(*a*), 8(*b*), 9(*a*), and 9(*b*).

Figure 11(*a*) shows the relationship between the normalized critical maximum contact pressure $P_{max,c}/H_b$ for the yield and the friction coefficient μ. It should be pointed out that the yield will appear firstly from the position where the minimum $P_{max,c}/H_b$

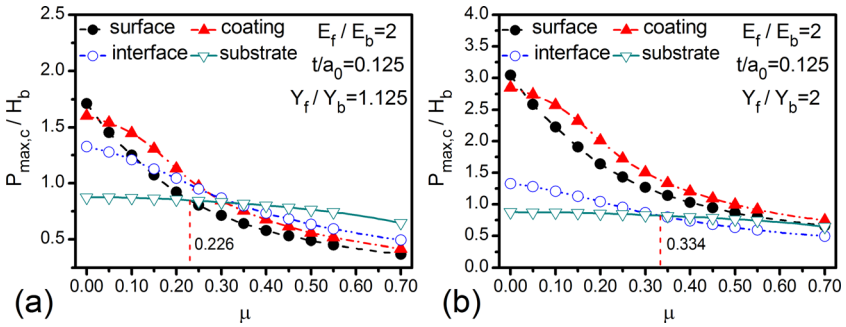

Fig. 11 Relationship between $P_{max,c}/H_b$ and μ, (*a*) $Y_f/Y_b = 1.125$ and (*b*) $Y_f/Y_b = 2$

places. So, for $Y_f/Y_b = 1.125$ according to Fig. 11(*a*), when the friction coefficient is lower than 0.226, the yield will initiate in the substrate (see Fig. 8(*a*)) while, when the friction coefficient is higher, the yield will initiate at the surface (see Figs. 8(*b*) and 9(*a*)). This means that, for the yield strength ratio of the coating to the substrate 1.125, the yield at the surface only initiates when the friction coefficient is larger than 0.226. This result will also verify the validity of the local yield map with a yielding at the surface under a low friction coefficient like 0.25 (see Fig. 8(*b*)). It is also interesting to discuss the transition of yielding positions from the substrate to the interface (see Figs. 8(*b*) and 9(*a*)) and when the yield in the substrate disappears from low friction to high friction (see Fig. 9(*a*)). As shown in Fig. 11(*b*), the relationship between the $P_{max,c}/H_b$ and the friction coefficient μ is presented. It is clear that yield will initiate in the substrate when the friction coefficient is lower than 0.334 (see Figs. 8(*a*) and 8(*b*)). But, once the friction coefficient is over that, the local yield initiation at the interface will dominate (see Fig. 9(*a*)). So it can be concluded that there must be a critical friction coefficient when local yield initiates from in the substrate to at the surface (see Fig. 11(*a*)) or from in the substrate to at the interface (see Fig. 11(*b*)), which leads to a gradual change instead of instant change between two local yield initiation states.

5 Conclusion

The yield of a three-dimensional substrate with a hard coating under sliding contact was solved, and the von Mises stress distributions in a hard coating for various combinations of coating thicknesses, friction coefficients, and elastic moduli of the coating and substrate were calculated. The positions of yield were found with the calculated results and the 3D-local yield maps were introduced in relation to the yield strength ratio of the coating to the substrate Y_f/Y_b and the ratio of the coating thickness to Hertzian contact radius t/a_0. Based on the presented results and discussions, the following conclusions can be drawn.

(1) 3D-local yield maps, which can be used to study and understand the yielding behavior of the hard coating intuitively and efficiently, is more exact and reliable than 2D-local yield maps.
(2) The positions of local yield initiation depend mainly on the friction coefficient in a coating-substrate system. When the friction coefficient is smaller than 0.25, the possibility of yield is below the surface. As the friction coefficient increased from 0.50 to 0.70, the position of yield is located at the surface or at the interface, especially in the case of friction coefficient 0.25 where a smaller zone with a yielding at the surface was found.
(3) There is a critical friction coefficient when local yield initiates from one position to the other, which leads to a gradual change instead of instant change between the two local yield initiation states. In the case of $Y_f/Y_b = 1.125$, the critical friction coefficient is 0.226 for controlling the yield position from in the substrate to at the surface. In the case of $Y_f/Y_b = 2$, the critical friction coefficient is 0.334 for dominating the yield initiation position to occur at the interface or in the substrate.

Acknowledgment

The authors would like to thank the National Nature Science Foundation of China under Grant Nos. 90923027 and 51050110137 as well as the Fundamental Research Funds for Central Universities for their support.

References

[1] Posti, E., and Niemiuen, I., 1989, "Influence of Coating Thickness on the TiN-Coated High Speed Cutting Tools," Wear, **129**, pp. 273–283.
[2] Holmberg, K., 1992, "A Concept for Friction Mechanisms of Coated Surface," Surf. Coat. Technol., **56**, pp. 1–10.
[3] Holmberg, K., Matthews, A., and Ronkainen, H., 1998, "Coatings Tribology—Contact Mechanisms and Surface Design," Tribol. Int., **31**(1–3), pp. 107–120.
[4] Treutler, C. P. O., 2005, "Industrial Use of Plasma-deposited Coatings for Components of Automotive Fuel Injection Systems," Surf. Coat. Technol., **200**, pp. 1969–1975.
[5] Erdemir, A., and Donnet, C., 2006, "Tribology of Diamond-Like Carbon Films: Recent Progress and Future Prospects," J. Phys. D: Appl. Phys., **39**, pp. R311–R327.
[6] Diao, D. F., Kato, K., and Hokkirigawa, K., 1994, "Fracture Mechanisms of Ceremic Coatings in Indentation," ASME J. Tribol. **116**, pp. 860–869.
[7] Oliveira, S. A. G., and Bower, A. F., 1996, "An Analysis of Fracture and Delamination in Thin Coatings Subjected to Contact Loading," Wear, **198**, pp. 15–32.
[8] Cheng, W., and Cheng, H. S., 1997, "Semi-Analytical Modeling of Crack Initiation Dominant Contact Fatigue Life for Roller Bearing," ASME J. Tribol., **119**, pp. 233–240.
[9] Bhomwick, S., Kale, A. N., Jayaram, V., and Biswas, S. K., 2003, "Contact Damage in TiN Coatings Steel," Thin Solid Films, **436**, pp. 250–258.
[10] Roman, K. Z., and Gabriel, R., 2010, "Stresses in Hard Coating Due to a Rigid Spherical Indenter on a Layered Elastic Half-Space," Tribol. Int., **43**, pp. 1592–1601.
[11] Keer, L. M., and Worden, R. E., 1990, "A Qualitative Model to Describe the Microchipping Wear Model in Ceramic Rollers," Tribol. Trans., **33**, pp. 411–417.
[12] Chen, S. Y., Farris, T. N., and Chandrasckar, S., 1991, "Sliding Microindentation Fracture of Brittle Materials," Tribol. Trans., **34**, pp. 161–168.
[13] Keer, L. M., and Kuo, C. H., 1992, "Cracking in a Loaded Brittle Elastic Half-Space," Int. J. Solids Struct., **29**, pp. 1819–1826.
[14] Bower, A. F., and Fleck, N. A., 1994, "Brittle Fracture Under a Sliding Line Contact," J. Mech. Phys. Solids, **42**, pp. 1375–1396.
[15] Ahmed, A., and Hadfield, M., 1999, "Failure Modes of Plasma Sprayed WC–15% Co Coated Rolling Elements," Wear, **230**(1), pp. 35–39.
[16] Zhou, K., Keer, L. M., Wang, Q. J., and Hua, D. Y., 2011, "Size Prediction of Particles Caused by Chipping Wear of Hard Coatings," Wear, **271**, pp. 1203–1206.
[17] Nowell, D., and Hills, D. A., 1988, "Contact Problems Incorporating Elastic Layers," Int. J. Solids Struct., **24**(1), pp. 105–115.
[18] King, R. B., and O'Sullivan, T. C., 1988, "Sliding Contact Stress Field Due to a Spherical Indenter on a Layered Elastic Half-space," ASME J. Tribol., **109**, pp. 223–231.
[19] Komvopoulos, K., Saka. N., and Suh, N. P., 1987, "The Role of Hard Layers in Lubricated and Dry Sliding," ASME J. Tribol., **109**, pp. 223–231.
[20] Komvopoulos, K., 1988, "Finite Element Analysis of a Layered Elastic Solid in Normal Contact With a Rigid Surface," ASME J. Tribol., **110**, pp. 477–485.

[21] Komvopoulos, K., 1989, "Elastic-Plastic Finite Element Analysis of Indented Layered Media," ASME J. Tribol., **111**, pp. 430–439.
[22] Plumet, S., and Dubourg, M. C., 1998, "A 3-D Model for a Multilayered Body Loaded Normally and Tangentially against a Rigid Body: Application to Specific Coatings," ASME J. Tribol., **120**, pp. 668–676.
[23] Stephens, L. S., Liu, Y., and Meletis, E. I., 2000, "Finite Element Analysis of the Initial Yielding Behavior of a Hard Coating-Substrate System With Functionally Graded Interface Under Indentation and Friction," ASME J. Tribol., **122**(2), pp. 381–387.
[24] Michler, J., and Blank, E., 2001, "Analysis of Coating Fracture and Substrate Plasticity Induced by Spherical Indentors: Diamond and Diamond-Like Carbon Layers on Steel Substrates," Thin Solid Films, **381**, pp. 119–134.
[25] Holmberg, K., Laukkanen, A., Ronkainen, H., and Wallin, K., 2005, "Tribological Analysis of Fracture in Thin Surface Coatings by 3D FEM Modeling and Stress Simulations," Tribol. Int., **38**, pp. 1035–1049.
[26] Lin, W., and Keer, L. M., 1989, "Three-Dimensional Analysis of Cracks in Layered Transversely Isotropic Media," Proc. R. Soc. London, Ser. A, **424**, pp. 307–322.
[27] Kuo, C. H., and Keer, L. M., 1995, "Three-Dimensional Analysis of Cracking in a Multilayered Composite," ASME J. Appl. Mech., **62**, pp. 273–281.
[28] Polonsky, I. A., and Keer, L. M., 2001, "Stress Analysis of Layered Elastic Solids With Cracks Using the Fast Fourier Transform and Conjugate Gradient Techniques," ASME J. Appl. Mech., **68**(5), pp. 708–714.
[29] Nogi, T., and Kato, T., 1997, "Influence of a Hard Surface Layer on the Limit of Elastic Contact—Part I: Analysis Using a Real Surface Model," ASME J. Tribol., **119**, pp. 493–500.
[30] Polonsky, I. A., and Keer, L. M., 1999, "A Numerical Method for Solving Rough Contact Problems Based on the Multi-Level Multi-Summation and Conjugate Gradient Techniques," Wear, **231**, pp. 206–219.
[31] Liu, S. B., Wang, Q., and Liu, G., 2000, "A Versatile Method of Discrete Convolution and FFT (DC-FFT) for Contact Analyses," Wear, **243**, pp. 101–111.
[32] Boucly, V., Nélias, D., Liu, S. B., Wang, Q. J., and Keer, L. M., 2005, "Contact Analyses for Bodies With Frictional Heating and Plastic Behavior," ASME J. Tribol., **127**, pp. 355–364.
[33] Wang, Z. J., Wang, W. Z., Wang, H., Zhu, D., and Hu, Y. Z., 2010, "Partial Slip Contact Analysis on Three-Dimensional Elastic Layered Half Space," ASME J. Tribol., **132**, p. 021403.
[34] Chen, W. W., Zhou, K., Keer, L. M., and Wang, Q. J., 2010, "Modeling Elasto-Plastic Indentation on Layered Materials Using the Equivalent Inclusion Method," Int. J. Solids Struct., **47**, pp. 2841–2854.
[35] Diao, D. F., Kato, K., and Hayashi, K., 1992, "The Local Yield Map of Hard Coating under Siding Contact," *Proceedings of the 19th Leeds-Lyon Symposium on Tribology*, Elsevier, Amsterdam, pp. 419–427.
[36] Diao, D. F., and Kato, K., 1994, "Interface Yield Map of a Hard Coating Under Sliding Contact," Thin Solid Films, **245**, pp. 115–121.
[37] Diao, D. F., and Ito, K., 1999, "Local Yield Map and Elastic-Plastic Deformation Map of Hard Coating With Lubricative Particles Under Sliding," Surf. Coat. Technol., **115**, pp. 193–200.
[38] Diao, D. F., and Kandori, A., 2006, "Finite Element Analysis of the Effect of Interfacial Roughness and Adhesion Strength on the Local Delamination of Hard Coating Under Sliding Contact," Tribol. Int., **39**, pp. 849–855.